SPE 63158

Inflow Performance Relationships for Gas Condensates

Fawzi M. Guehria, SPE, Schlumberger Integrated Project Management

Copyright 2000, Society of Petroleum Engineers Inc.

This paper was prepared for presentation at the 2000 SPE Annual Technical Conference and Exhibition held in Dallas, Texas, 1–4 October 2000.

This paper was selected for presentation by an SPE Program Committee following review of information contained in an abstract submitted by the author(s). Contents of the paper, as presented, have not been reviewed by the Society of Petroleum Engineers and are subject to correction by the author(s). The material, as presented, does not necessarily reflect any position of the Society of Petroleum Engineers, its officers, or members. Papers presented at SPE meetings are subject to publication review by Editorial Committees of the Society of Petroleum Engineers. Electronic reproduction, distribution, or storage of any part of this paper for commercial purposes without the written consent of the Society of Petroleum Engineers is prohibited. Permission to reproduce in print is restricted to an abstract of not more than 300 words; illustrations may not be copied. The abstract must contain conspicuous acknowledgment of where and by whom the paper was presented. Write Librarian, SPE, P.O. Box 833836, Richardson, TX 75083-3836, U.S.A., fax 01-972-952-9435.

Abstract

In this work, we describe a fast scheme to obtain time-dependent IPR curves for a depleting gas-condensate well without resorting to the use of simulation.
The model reflects the flowing characteristics inside the reservoir. In addition, it is self-checking and consistent with the overall analysis of gas-condensate reservoir behavior.
We also investigate the adequacy of reservoir material balance for gas-condensates to generate the IPR curves for a depleting gas-condensate well.
Transient effects are not considered in this work.

Inflow Performance Relationships (IPR's) are a critical element in the design of new wells and in the monitoring and optimization of existing producing wells. In addition to Vogel-type relationships, various IPR models for different well geometry and different flow regimes have been presented. Generally, these models take advantage of analytical solutions for single-phase oil and for single-phase gas, to generate a flow rate profile with flowing pressure as a parameter.
For gas-condensate wells, standard dry-gas deliverability equations based on isochronal testing have always been used as IPR models. Unfortunately, due to severe deliverability reduction caused by condensate blockage, this approach is inadequate and usually leads to erroneous results.

In reality, the pressure drop that occurs in gas-condensate reservoirs operating below dew-point, is affected by up to three zones, i.e. 1) inner zone where both phases, gas and free condensate, are flowing, 2) middle zone where two phases co-exist but only gas is mobile and 3) outer zone where only the single phase gas is flowing.

We verified the method with synthetic examples and good agreement was achieved in all cases.

Introduction

Well construction design and well performance diagnosis and optimization heavily rely on well deliverability modeling, which combines tubular hydraulic calculations with a reservoir deliverability model. The latter is represented by a curve, which relates flow rates to flowing bottomhole pressures for a given fixed reservoir pressure.
Gilbert [1] introduced the concept of *Inflow Performance* Relationship *(IPR) of a well.* Later, Vogel[2] established an empirical relationship between production rate and flowing bottomhole pressure in solution gas drive reservoirs. His work is based on Weller's[3] approximations, which assume that the tank-oil de-saturation rate is the same at every point in the reservoir at any given time. Vogel relation assumes the following form:

$$\frac{q_o}{q_{o,\max}} = 1 - 0.2\left(\frac{p_{wf}}{\overline{p}}\right) - 0.8\left(\frac{p_{wf}}{\overline{p}}\right)^2 \qquad (1)$$

where q_o is the oil producing rate corresponding to a given flowing bottomhole pressure, p_{wf} . $\overline{p}$ is a fixed reservoir pressure and $q_{o,\max}$ is the maximum producing rate corresponding to a zero flowing bottomhole pressure.
For wells producing below bubble point, Fetkovich used the following generalized equation:

$$q_o = C\frac{\overline{p}}{p_i}\left(\overline{p}^2 - p_{wf}^2\right)^n \qquad (2)$$

where, p_i is the initial reservoir pressure, and C and n are constants determined in isochronal testing.
Other relations based on steady-state and pseudo-steady-state solutions for single phase have also been used to compute the productivity index (PI) of wells of various geometry, i.e., vertical hole, horizontal drain, multi-branched drains, etc.

Gas Condensates

Gas-condensate wells behavior is unique in a sense that it is characterized by a rapid loss of well productivity. Generally, when the flowing bottomhole pressure drops below the dew point, a region of high condensate saturation builds up near the wellbore, causing lower gas deliverability mainly due to a reduction in gas permeability. Numerous authors investigated the phenomenon, which Muskat[4] referred to as a condensate-blockage. He designed a method to calculate the radius of this blockage, which grows with time. This method requires knowledge of the gas rate, reservoir and PVT properties. Later, Fetkovitch[5] represented this condensate blockage by associating a time-dependent skin to the standard gas rate equation.

The well deliverability loss for gas-condensate wells was later confirmed through numerical simulation by Kniazeff and Naville[6] and Eilerts et al[7,8]. Similarly, Gondouin et al.[9] studied the importance of condensate blockage by use of radial black-oil numerical simulation.

O'Dell and Miller[10] introduced a pseudopressure function in the gas rate equation to describe the effect of condensate blockage. Their work clearly shows that minor condensate blockage can significantly reduce well deliverability. Fussell[11] was first to investigate the well productivity loss via an Equation-of-state (EOS) based compositional simulator. Jones, Raghavan and Vo[12] primarily focused on the effect of condensate blockage on the pressure transient response observed during drawdown and buildup periods. Their analytical work makes use of results from an EOS based three component compositional radial simulator. Concerning the boundary-dominated flow period, they confirmed that the pseudopressure used by Fussell is valid at all times. This reservoir integral pseudopressure is evaluated only if the pressure and saturation profiles along the reservoir are established a priori via a simulation run.

Well Deliverability Equation

Equations for two-phase flow were first solved by Muskat and Meres[13] for a few special cases. Evinger and Muskat[14] studied the effect of multiphase flow on productivity index of a solution-gas drive well and examined the steady-state radial flow of oil and gas in a porous medium. Under conditions of steady-state radial flow, the oil phase is given by

$$q_o = \frac{kh}{141.2\ln(re/rw)} \int_{p_{wf}}^{p_e} \frac{k_{ro}(S_o)}{\mu_o B_o} dp \qquad (3)$$

Levine and Prats[15] extended the understanding of solution-gas drive reservoirs and well behavior. They showed that, if it is assumed that the decline rate of stock-tank oil in place is constant everywhere, then the equation governing flow of oil in radial coordinates can be directly integrated to give

$$\int_{p}^{p_e} \frac{k_{ro}(S_o)}{\mu_o B_o} dp = \frac{141.2 q_o}{kh}\left[\frac{1}{2}\left(\frac{r^2 - r_w^2}{r_w^2}\right) - 2Ln\frac{r}{r_e}\right] \qquad (4)$$

As in the case of steady-state, a relation between saturation and pressure is needed to calculate the integral on the left-hand side of Eq. (4). In addition, the pressure p_e and the corresponding saturation would have to be known.

By analogy to solution-gas drive reservoirs, an equation may be derived for depleting gas-condensate reservoirs. It is expressed as

$$q_g = C \int_{p_{wf}}^{p_R} \left(\frac{k_{rg}}{\mu_g B_g} + R_s \frac{k_{ro}}{\mu_o B_o}\right) dp \qquad (5)$$

where

$$C = \frac{kh}{141.2\left[\ln\left(\frac{r_e}{r_w}\right) - \frac{3}{4} + s\right]} \qquad (6)$$

In Eq. (6), s is the damage skin. Note that the pressure loss due to condensate blockage is implicitly accounted for in the method by which the pseudopressure integral is evaluated.

To calculate the pseudo-steady-state rate equation (5), . Fevang and Whitson[16] proposed a method to model the deliverability of gas-condensate wells. In addition to the pressure/volume/temperature (PVT) black-oil or compositional properties and the gas/oil relative permeability, the producing gas-oil ratio (GOR) is required for each reservoir pressure p_R.

Fevang and Whitson identified the existence, at any time of depletion, of one, two or three flow regions, depending on the values of the flowing bottomhole pressure and the reservoir pressure.

If the flowing bottomhole pressure is above the initial in-situ fluid dew point, the whole reservoir is single phase and Eq. (5) becomes a standard gas rate equation with $k_{ro} = 0,$ and $k_{rg} = k_{rg}(S_{wi}),$ where S_{wi} is the irreducible water saturation.

If the flowing bottomhole pressure is below dew point, then the reservoir may contain three flow regions. Region 1 is defined as a zone closer to the inner near-wellbore where both gas and oil flow simultaneously. Outward into the reservoir, Region 2 contains a condensate buildup where only gas is flowing. Finally, contiguous to Region 2, Region 3, which extends to the limits of the reservoir, exists only if the reservoir pressure is higher than the dew point pressure. The size of each region changes with time as the reservoir depletes. Fevang and Whitson suggested that, given the flowing

bottomhole pressure, producing GOR and reservoir pressure, the rate given by Eq. (5) is computed by splitting up the pseudopressure integral into three integrals. The limits of those integrals are the pressures at the boundaries of each region, i.e., p_{wf} , p^* , p_{dew} , and p_R . p^* is the pressure at the outer boundary of Region 1.
The pseudopressure integrals defining each region are evaluated by use of the PVT curves and the relative permeability modified Evinger-Muskat approach.
One of the major findings in this work is that the primary cause of reduced well deliverability within Region 1 is k_{rg} as a function of $(k_{rg}/k_{ro})(p)$ which, is computed via the definition of the producing GOR, as expressed by Eq. (C1). It was also found that critical oil saturation has no effect on gas-condensate well deliverability.
The authors discussed the phase behavior characteristics in each region and noted that Region 1 behaves like a constant composition expansion (CCE) cell, whereas Region 2 acts like a constant volume depletion (CVD) cell. Based on this, they argued that the produced wellstream has the same composition as the single-phase gas entering Region 1 and thus the flowing GOR must be constant throughout Region 1. The pressure at the outer boundary of Region 1, p^*, is defined as the pressure at which the producing GOR, R, is the inverse of the solution condensate-gas ratio (CGR), R_v , which is provided in the PVT table.
Unfortunately, this model requires that these values be established a-priori by numerous simulation runs and tabulated for each reservoir pressure.

New Inflow Performance Relationships Model

Discussion

Practices in field development and production management usually involve field design strategies and continual monitoring of surface facility network, reservoir and wells. Well management includes regular well testing and the use of a wide variety of diagnosis and prediction tools.
IPR modeling combined with tubing intake analysis are a very useful element in a strategy for wells capital and operating expenditures. The construction of a new well should include a completion designed for optimum initial fluid rates and should also accommodate all future flowing condition changes. Well modeling is also a standard tool for the monitoring of well productivity and for allowing the field engineer to choose a proper remedial job, e.g., stimulation, work-over, etc., in order to rehabilitate the optimum well performance.
On a larger scale, it is also imperative to be able to optimize a well performance within the constraints of the surface facility network. For that, a prediction on rates and producing GOR's is critical for continuous global field production optimization. This is achieved via a planned wellhead control program for each well connected through the manifold.

We recall that during production, gas-condensate wells main flowing characteristics are as follows:
At the start of production of a well from a gas-condensate reservoir initially above saturation pressure, the produced condensate yield (CGR) is at its maximum, i.e., the value of the solution CGR at dew point pressure. Similarly, the observed producing GOR is exactly the inverse of the producing CGR. This is mainly due to the fact that the reservoir is operating above the dew point and that the condensate blockage zone is not large enough to reduce the recovery of liquids which, remain mainly in the condensate rich gas-phase. However, during depletion, as the pressure drops, a condensate region builds up in the reservoir area where pressure is below dew point, causing a reduction in well deliverability. This translates into a continual decrease in the produced condensate yield (produced CGR) and a continual increase in the producing GOR. Normally, a relatively large skin observed in transient analysis reflects this productivity impairment. Note that the high skin may also include other effects, e.g., near-wellbore mechanical damage, spherical flow due to possible partial penetration, or other non-darcy effects due to turbulence. It is of paramount importance to properly identify the different near-wellbore effects that are causing the productivity index (PI) reduction, before an expensive intervention on the well is recommended and executed.

Generating proper time-dependent IPR curves for a gas-condensate well is important in the identification and quantification of well productivity losses in addition to determining the right surface control parameters to achieve optimum production at the manifold-separator level.
Time-dependent IPR curves for gas-condensate wells may be generated by use of a gas deliverability model provided the producing GOR is known for each reservoir pressure.

Depending on the purpose of the analysis, IPR curves for gas-condensate wells may be expressed in terms of gas flow rates. However, if the reservoir fluid is rich, and the CGR is relatively high, then predicting condensate flow rates might be a more suitable approach. For this case, the analog of Eq. (5), i.e., the condensate flow rate is given by

$$q_o = C \int_{p_{wf}}^{p_R} \left(\frac{k_{ro}}{\mu_o B_o} + R_v \frac{k_{rg}}{\mu_g B_g} \right) dp \qquad (7)$$

The total flow rate may be expressed as

$$q_t = \alpha q_o + (1-\alpha) q_g \qquad (8)$$

where $\alpha = 1$ for condensate flow rate, $\alpha = 0$ for gas flow rate and $\alpha = 0.5$ for half the total flow rate. This is particularly convenient for generalized computer coding purposes.
We recall that if a well produces with a flowing bottomhole

pressure lower than the dew point, the producing GOR is a monotonically increasing function of reservoir pressure, i.e., a one-to-one relationship between producing GOR and pressure exists as soon as a two-phase flow region develops within the reservoir.
Evaluating Eq. (5) or Eq. (7) via a well deliverability model, e.g., Fevang and Whitson model, requires knowledge of producing GOR for each reservoir pressure.

Material Balance

To construct a table of producing GOR versus reservoir pressure, we investigated the option of using a reservoir material balance (MB) technique for gas-condensate reservoirs, as laid out in Appendix D. We recall the major assumptions inherent to a material balance model for gas-condensate reservoirs:

1. If a well is producing from an undersatured reservoir, with a flowing bottomhole pressure lower than the in-situ fluid dew point, the material balance technique is not applicable, i.e., the reservoir pressure may remain above dew point, whereas a two-phase zone starts building up, causing the producing GOR to increase.
2. Material balance assumes that the reservoir pressure and the phase saturations are uniform throughout the reservoir at all times. This implies that only one region exists, e.g., a two-phase region where a phase flow is dictated by a given relative permeability set input; e.g., for oil saturations below the critical oil saturation, S_{oc}, it is assumed that only leaner gas is flowing to the wellbore, regardless of pressure level.

Integrated Method

In this work, we investigate the idea of developing a fast scheme to obtain time-dependent IPR curves for a depleting gas-condensate well without resorting to the use of simulation. The model reflects the flowing characteristics inside the reservoir. In addition, it is self-checking and consistent with the overall analysis of gas-condensate reservoir behavior.

The framework of our approach is the basic two-component flow equations in porous medium, as given by Eq. (A1) and Eq. (A2). These equations respectively relate the rate of change of mass of gas and of oil stored in a unit volume of the reservoir at a chosen location, to the transport terms at the same location. We will show that our model integrates both elements for consistency, in the same spirit as a simulator numerical scheme does iteratively.

It is observed in simulation that after the well stabilizes, in-situ flowing GOR gradients are negligible within the region where both phases are flowing. Appendix A gives an analytical/physical explanation of this behavior.

Furthermore, it is shown in Appendix B that the in-situ flowing GOR within the region where both phases are flowing, can be expressed as

$$R = \frac{\dfrac{\partial}{\partial p}\left(\dfrac{S_g}{B_g} + R_s \dfrac{S_o}{B_g}\right)}{\dfrac{\partial}{\partial p}\left(\dfrac{S_o}{B_o} + R_v \dfrac{S_g}{B_g}\right)} \tag{9}$$

Eq. (9) represents the ratio of the rate of change of mass of gas to the rate of change of mass of oil. It can further be expanded as

$$R = \frac{\left(-\dfrac{1}{B_g} + \dfrac{R_s}{B_o}\right)\dfrac{dS_o}{dp} - S_o\left[\dfrac{d\left(\dfrac{1}{B_g}\right)}{dp} - \dfrac{1}{B_o}\dfrac{dR_s}{dp} - R_s\dfrac{d\left(\dfrac{1}{B_o}\right)}{dp}\right]}{\left(\dfrac{1}{B_o} - \dfrac{R_v}{B_g}\right)\dfrac{dS_o}{dp} + S_o\left[\dfrac{d\left(\dfrac{1}{B_o}\right)}{dp} - \dfrac{1}{B_g}\dfrac{dR_v}{dp} - R_v\dfrac{d\left(\dfrac{1}{B_g}\right)}{dp}\right]} \tag{9'}$$

Eq. (9') shows that the in-situ flowing GOR can be estimated at a new pressure level $(p+1)$, in Region 1, provided the saturation profile is known at the same pressure level. The PVT properties $B_o, \mu_o, B_g, \mu_g, R_v$, and R_s are readily available within the depletion pressure range as provided by the PVT curves. All derivatives may be approximated by chord slopes.

This suggests an iterative scheme where, given a fixed reservoir pressure, p_R, and an assumed producing GOR value, the flow rates as given by Eq. (5) or Eq. (7) can be computed for a specified flowing bottomhole pressure. With Region 1 being defined via the calculation of the pseudopressure integral as suggested by Fevang and Whitson, the resulting saturation profile and the PVT properties evaluated at a pressure value prevailing within Region 1, are then used to compute the GOR value as expressed by Eq. (9'). If this value does not compare with the originally assumed value used in the evaluation of the pseudopressure integral, then the process is repeated with a new producing GOR value until both of the values agree within a certain tolerance. Normally, if the gas rate at the previous iteration is larger than the newly computed rate, then we decrease the producing GOR value, else, we increase it.
For the next reservoir pressure, the producing GOR value required to start the iteration is the value found at the previous pressure, augmented by a certain incremental value.

Usually, IPR curves are used when the well drainage volume is established via an acre spacing planning. Transient effects are not considered in this work. We will assume that for an initial reservoir pressure above the dew point, the IPR curve is generated with a producing GOR equal to the inverse of the solution CGR defined at the dew point.

This scheme offers consistency as it integrates the transport terms and the accumulation terms appearing respectively in both sides of the equations governing fluid flow within Region 1, so that mass balance is preserved.

Results

We tested the idea of generating time-dependent IPR curves via the method described above and compare the results with those generated by a Beta model (modified black-oil simulator). Fluid properties are assumed to be function of pressure only, so that flow in the reservoir may be adequately described by a $\beta-$model.

Our $\beta-$model built for that purpose is based on the numerical solution of the flow equations (A1) and (A2) subject to appropriate initial and boundary conditions, with the Laplacian operator defined in cylindrical coordinates.
The simulator considers isothermal flow to a cylindrical well which, fully or partially penetrates a cylindrical reservoir. Gravity is accounted for, whereas capillary effects are assumed to be negligible. The reservoir is bounded above and below. At the external reservoir radius, i.e., at $r = r_e$, the boundary condition imposed, could either be a no-flow boundary (sealed by impermeable rock) or a constant pressure boundary (influx from outside the reservoir). Only hydrocarbon fluids are present in the reservoir – any water present is assumed to be incompressible and immobile and no account is taken of its presence. The permeability field could be anisotropic, i.e., $k_z \neq k_r$. Reservoir compaction is also accounted for as an option with permeability and porosity being function of pressure.
As is standard in reservoir simulation, the skin zone is modeled as a zone of altered permeability (i.e., $k_s \neq k_r$) concentric with the wellbore in accordance with Hawkins (12) formula:

$$s = \left(\frac{k_s}{k_r} - 1\right) Ln\left(\frac{r_s}{r_w}\right) \qquad (7)$$

Under the above assumptions, flow to the wellbore can be either spherical or purely radial.
Fluid PVT properties and relative permeability are input as discrete tabulated data; PVT properties above the saturation pressure are functions of both pressure and saturation pressure. Properties at a particular value of pressure or saturation are obtained by linear interpolation between tabulated data.

For the purpose of validation of numerical results with analytical theory, all cases tested assume that the reservoir is homogeneous, isotropic and that the flow is purely radial. In addition, the reservoir is sealed at the outer boundary.

We considered numerous simulations runs with different fixed flowing bottomhole pressures. In all runs, we assumed a reservoir permeability of 50 md, porosity of 8 % and a single layer with thickness of 15.5 ft. The wellbore radius was set at 0.33 ft, while the external reservoir radius was 1000 ft. Reservoir properties are summarized in Table 1. The relative permeability set is given in Table 2. Two types of fluids were considered: a rich and a lean gas-condensate fluids with a maximum CGR of 148 Stb/MMscf and 55 STB/MMscf, respectively. The key reservoir fluid properties are shown in Table 3.
Fig. 1 depicts the numerical simulator results showing reservoir pressure decline during depletion of the reservoir containing the rich gas A, whereas Fig. 2 shows the CGR profile for the same conditions. Although not shown in Fig. 2, the CGR maintains an approximatively constant value equal to the initial solution CGR, during the early part of production. The producing GOR values were tabulated for each simulation run, then used in the deliverability equation, i.e., Eq. (7).

We also investigated the case where the produced GOR values are computed as function of pressure via reservoir MB calculations for gas-condensate reservoirs. The reservoir MB balance assumes the existence of one region at most, at any time of depletion. Before the critical oil saturation is reached, the whole reservoir contains a single region, Region 2, where both phases coexist, but only gas is flowing. Above the critical oil saturation, the whole reservoir acts as Region 1, i.e., both phases are flowing throughout the reservoir.
The producing GOR profiles from the fine grid simulator and the reservoir MB is shown in Fig. 3. Simulation was performed with a constant flowing bottomhole pressure equal to 2000 psia and the run was conducted until a low rate limit was reached at a reservoir pressure slighly higher than 2000 psia. However, the reservoir MB predicts results within the whole PVT properties pressure range. Fig. 3 shows that both profiles coincide perfectly at early time of depletion. It is worth noting that the reservoir MB results are independent of pressure gradients within the reservoir and thus, the producing GOR is not affected by the pressure drawdown imposed on the well, but rather by reservoir pressure. Figs 4 and 5 depict the oil and gas recovery, respectively, as computed by fine grid reservoir simulation and reservoir MB. The oil recovery profiles shows an increasing discrepency between both methods. This is mainly due to the fact that the fine grid simulator accounts for all regions within the reservoir, whereas the reservoir MB assumes a single contributing region at a time.

Fig. 6 shows the IPR curves generated for the case of the rich gas-condensate fluid A. Good agreement was achieved between the prediction values of our model and those based on

fine grid simulation, at all times. Although, not shown, the producing GOR's profiles from simulation runs are consistent with those predicted in the integrated model.

We then used the producing GOR values generated by the reservoir MB, to evaluate Eq. (7) for each reservoir pressure and flowing bottomhole pressure. Note that at pressions above dew point, the reservoir MB is not applicable. The match is good at higher pressures, but start degrading at low pressures.

Fig. 7 shows a set of IPR curves generated for lean gas B, by use of reservoir MB results, fine grid simulation and the integrated method. All results are consistent due to the fact that condensate blockage is not as prevalent and that all methods reproduce the fine grid simulation results.

Field Application

Normally, in a routine well management process, wellhead data is collected on a regular basis. These data include choke sizes, wellhead pressures, flow rates and producing GOR measured at a preset mobile test separator. Also, wells are shut in on a regular basis for pressure measurements during a buildup phase. The reservoir properties extracted from the pressure transient analysis are reservoir pressure, flow capacity, kh, and skin, s.
However, in reality of actual cost control measures, field data collection programs may not be always adequate for properf well management. Sometimes, data is recorded at different times with different flowing conditions. In other cases, only wellhead pressure and at best, flowing gradient within the tubulars are recorded. In other instances, some high PI wells are rarely shut in for pressure buildup analysis. In this case, skin and reservoir pressure may not be available to assess the well deliverability. The analyst is then confronted with providing a well diagnosis with limited data.
IPR curves may be of great help to reduce uncertainties on the missing parameters.

A gas-condensate well in West Texas producing in a 200 acre spacing was tested on a regular basis. The initial condensate yield was 90 STB/MMscf with a maximum CVD liquid dropout of 7 %. A reservoir MB model as described in Appendix D was used to estimate reservoir pressure profile, knowing the recovery factor and producing GOR's. IPR curves and hydraulic lift curves were generated and graphed on the same plot. The test points available were reproduced by varying the mechanical skin. Fig. 8 depicts the match obtained for the two test points availalble and the skin determined is in the range of 6.

Conclusions

In this paper, we presented a novel approach to generate IPR curves for depleting gas-condensate reservoirs. We also investigated the use of the reservoir MB results in the computation of the well deliverability equation in the spirit of the Fevang and Whitson gas-condensate well behavior description. The following summarizes our results:

- For rich gas-condensate, we describe a consistent iterative integrated method to generate IPR curves.
- For lean gas condensates, GOR values from the reseroir MB model are adequate to achieve good results.
- The initial solution CGR can be used at pressures close to the initial dew-point.
- Producing GOR's depend on reservoir pressure and not on pressure drawdown imposed on the well.
- Field tests should also be used to calibrate the well deliverability by running sensitivities on the various parameters contained in Eq. (5) or Eq. (7).

Appendix A

The flow of oil and gas in terms of black-oil PVT, in a heterogeneous porous medium, neglecting gravity and capillary forces, are given by the following equations:

Oil

$$C_1\vec{\nabla}.\left[\left(\frac{k_{ro}}{\mu_o B_o}+R_v\frac{k_{rg}}{\mu_g B_g}\right)[k]\vec{\nabla}p\right]=\frac{\partial}{\partial t}\left[\phi\left(\frac{S_o}{B_o}+R_v\frac{S_g}{B_g}\right)\right] \quad \text{(A1)}$$

Gas

$$C_1\vec{\nabla}.\left[\left(\frac{k_{rg}}{\mu_g B_g}+R_s\frac{k_{ro}}{\mu_o B_o}\right)[k]\vec{\nabla}p\right]=\frac{\partial}{\partial t}\left[\phi\left(\frac{S_g}{B_g}+R_s\frac{S_o}{B_o}\right)\right] \quad \text{(A2)}$$

where $\vec{\nabla}$ denotes the gradient,

$$\vec{\nabla}=\frac{\partial}{\partial x}+\frac{\partial}{\partial y}+\frac{\partial}{\partial z}$$

and the right-hand side of Eqs. (A1)-A(2) represent the partial derivative of the quantities with respect to time.

The flowing gas-oil ratio R is defined as:

$$R = \frac{\left(\frac{k_{rg}}{\mu_g B_g} + R_s \frac{k_{ro}}{\mu_o B_o}\right)[k]\vec{\nabla}p}{\left(\frac{k_{ro}}{\mu_o B_o} + R_v \frac{k_{rg}}{\mu_g B_g}\right)[k]\vec{\nabla}p} \quad \text{(A3)}$$

Using Eq. (A3) in the gas equation (A2) and expanding yields:

$$C_1 R\vec{\nabla}.\left[\left(\frac{k_{ro}}{\mu_o B_o} + R_v \frac{k_{rg}}{\mu_g B_g}\right)[k]\vec{\nabla}p\right] + C_1\left(\frac{k_{ro}}{\mu_o B_o} + R_v \frac{k_{rg}}{\mu_g B_g}\right)[k]\vec{\nabla}R = \frac{\partial}{\partial t}\left[\phi\left(\frac{S_g}{B_g} + R_s \frac{S_o}{B_o}\right)\right] \quad \text{(A4)}$$

For the oil phase, Darcy's law is given by

$$1.127\times10^{-3} A\left(\frac{k_{ro}}{\mu_o B_o} + R_v \frac{k_{rg}}{\mu_g B_g}\right)[k]\vec{\nabla}p = q_o(\vec{x},t) \quad \text{(A5)}$$

Combining Eq. (A5) with Eq. (A4) and rearranging give

$$\frac{C_1}{1.127\times10^{-3} A}\vec{\nabla}R = \frac{\frac{\partial}{\partial t}\left[\phi\left(\frac{S_g}{B_g} + R_s \frac{S_o}{B_o}\right)\right]}{Rq_o(\vec{x},t)} - \frac{\frac{\partial}{\partial t}\left[\phi\left(\frac{S_o}{B_o} + R_v \frac{S_g}{B_g}\right)\right]}{q_o(\vec{x},t)} \quad \text{(A6)}$$

The right-hand side of Eq. (A6), respectively account for the rate of change of mass of gas and oil stored in a unit volume of the reservoir at some location (x,y,z). The denominators are respectively the mass flow rates of gas and oil through the location (x,y,z). At long times (close to a sink, i.e., a producing well), the time derivative terms become smaller as more mass is being transferred from further out in the reservoir to the well, whereas the denominator terms remain relatively large. This implies that the right-hand side of Eq. (A6) goes to zero at large times ("steady-state"), so that at long times

$$\vec{\nabla}R = \vec{0} \quad \text{(A7)}$$

Eq. (A7) shows that during stabilized flow, the flowing gas-oil ratio is the same throughout the zone where both oil and gas are flowing.

Appendix B

Furthermore, if we use Eq. (A1) into Eq. (A4), with $\vec{\nabla}R = 0$, we obtain

$$R = \frac{\frac{\partial}{\partial t}\left[\phi\left(\frac{S_g}{B_g} + R_s \frac{S_o}{B_o}\right)\right]}{\frac{\partial}{\partial t}\left[\phi\left(\frac{S_o}{B_o} + R_v \frac{S_g}{B_g}\right)\right]} \quad \text{(B1)}$$

Assuming constant porosity and using the chain rule for derivatives,

$$\frac{dx}{dt} = \frac{dx}{dp}\frac{dp}{dt}$$

Eq. (B1) may be rewritten as

$$R = \frac{\frac{\partial}{\partial p}\left(\frac{S_g}{B_g} + R_s \frac{S_o}{B_o}\right)}{\frac{\partial}{\partial p}\left(\frac{S_o}{B_o} + R_v \frac{S_g}{B_g}\right)} \quad \text{(B2)}$$

Appendix C

Eq. (A3) can be rewritten as

$$\frac{k_{rg}}{k_{ro}}(p) = \left(\frac{R - R_s}{1 - R_v R_s}\right)\left(\frac{\mu_g B_g}{\mu_o B_o}\right) \quad \text{(C1)}$$

It is readily shown that Eq. (C1) can be expressed in terms of the oil relative volume during a constant composition expanson (CCE), i.e.,

$$\frac{k_{rg}}{k_{ro}}(p) = \left(\frac{1}{V_{roCCE}} - 1\right)\frac{\mu_g}{\mu_o} \quad \text{(C2)}$$

Combining Eqs. (6) and (7) yield

$$V_{roCCE} = \frac{1}{\left[1 - \frac{(R - R_s)}{(1 - R_v R_s)}\frac{B_g}{B_o}\right]} \quad \text{(C3)}$$

Appendix D

Tank-type models and gridded models use similar continuity

(material balance) principles. For a two-phase (gas/oil) gridded model omitting gravity and capillary forces, the oil phase and gas phase partial differential differential equations that combine Darcy-law flow and continuity are Eq. (D1) and Eq. (D2). These equations are in Darcy units.

Oil

$$\vec{\nabla}.\left[\left(\frac{kk_{ro}}{\mu_o B_o}+R_v\frac{kk_{rg}}{\mu_g B_g}\right)\vec{\nabla}p\right]=\phi\frac{\partial}{\partial t}\left(\frac{S_o}{B_o}+R_v\frac{S_g}{B_g}\right)-q_{ov} \quad \text{(D1)}$$

Gas

$$\vec{\nabla}.\left[\left(\frac{kk_{rg}}{\mu_g B_g}+R_s\frac{kk_{ro}}{\mu_o B_o}\right)\vec{\nabla}p\right]=\phi\frac{\partial}{\partial t}\left(\frac{S_g}{B_g}+R_s\frac{S_o}{B_o}\right)-q_{gv} \quad \text{(D2)}$$

The left-hand sides of Eq. (D1) and Eq. (D2) represent, repectively, the transport terms of oil (free oil + oil in gas phase) and gas (free gas + gas in solution) in the reservoir (between blocks in a gridded model) and would be zero for a tank-type (one-block) model. The right-hand side terms of the same equations represent, respectively, the oil and gas accumulation and production.

The corresponding equations for a tank-type model are obtained by noting that the left-hand sides of Eq. (D1) and Eq. (D2) are zero for the tank-type model. Deleting the left-hand side of each equation, multiplying by the bulk volume, and changing to oilfield units yield

$$V_p\frac{\partial\overline{\alpha}}{\partial t}=q_o \quad \text{(D3)}$$

and

$$V_p\frac{\partial\overline{\beta}}{\partial t}=q_g \quad \text{(D4)}$$

where $\overline{\alpha}$ and $\overline{\beta}$, defined by Eq. (D5) and Eq. (D6) and represent the whole reservoir

$$\alpha=\left(\frac{S_o}{B_o}+R_v\frac{S_g}{B_g}\right) \quad \text{(D5)}$$

$$\beta=\left(\frac{S_g}{B_g}+R_s\frac{S_o}{B_o}\right)$$

Integrating Eq. (D3) and Eq. (D4) and rearranging yield

$$\frac{N_p}{N}=1-\frac{S_o\left[B_{oi}\left(B_g-R_vB_o\right)\right]+B_{oi}R_vB_o}{B_oB_g} \quad \text{(D6)}$$

and

$$\frac{G_p}{G}=\frac{N_p}{N}R\left(\frac{1}{R_{si}}\right) \quad \text{(D7)}$$

The producing GOR, R, expressed in scf/STB, is defined as

$$R=\frac{R_s+\left(\frac{k_{rg}/\mu_gB_g}{k_{ro}/\mu_oB_o}\right)}{1+R_v\left(\frac{k_{rg}/\mu_gB_g}{k_{ro}/\mu_oB_o}\right)} \quad \text{(D8)}$$

Eq. (D6) and Eq. (D8) represent two equations with two unknowns, S_o and R, for a given reservoir pressure. For material balance calculation purposes, we assume that the relative permeability is a function of saturation over the whole reservoir. This suggests an iterative process, which should yield a value of producing GOR for each depleting reservoir pressure.

Acknowledgements

The author would like to thank Schlumberger Oilfield Services for permission to publish this work.

Nomenclature

A = Area, ft^2
B_{gd} = Dry gas volumetric factor, Rb/Scf
B_o = Oil formation volume factor Rb/Stb
B_{oi} = Initial oil formation volume factor, Rb/Stb
C = Gas rate constant
G = Original gas-in-place, ft^3
G_p = Cumulative gas produced, ft^3
J = Productivity index
k = Absolute rock permeability, md
k_r = Radial permeability, md
k_s = Permeability of the skin zone, md
k_{ro} = Oil relative permeability
k_{rg} = Gas relative permeability
Np = Cumulative oil production, Stb
N = Original oil in-place, Stb
p_{dew} = Dew-point pressure, psia
p_i = Initial reservoir pressure, psia
p_{wf} = Flowing bottomhole pressure, psia
p_R = Reservoir pressure, psia
p_e = Pressure at external boundary, psia
q_t = Total flow rate, Stb/Day

q_o = Oil flow rate, Stb/Day
q_g = Gas flow rate, Mscf/Day
r_w = Wellbore radius, ft
r_s = Skin near-wellbore radius, ft
r = External reservoir radius, ft
R = Producing GOR, Scf/STB
R_s = Solution GOR, Scf/STB
R_v = Solution condensate-gas ratio, MMscf/STB
S_o = oil saturation, fraction
S_g = gas saturation, fraction
S_{oc} = critical oil saturation, fraction
S_{wi} = connate water saturation
V_p = Pore volume, ft^3
μ_o = oil viscosity , cp
μ_g = gas viscosity , cp
V_{roCCE} = Relative oil volume in constant composition experiment
V_{roCVD} = Relative oil volume in constant volume depletion experiment
CVD = Constant volume depletion
CCE = Constant composition expansion
MB = Material balance

Greek Symbols

$\vec{\nabla}$ = Laplacian
∂ = Partial derivative
ϕ = porosity
μ = viscosity

Subscripts and Superscripts

c = critical
dew = dew point
o = oil
g = gas
p = pore
r = radial or relative
s = skin or solution
v = volatility
w = wellbore
wf = flowing bottomhole

SI Metric Conversion Factors

Acre × 4.046873	E – 01 = ha
°API 141.5/(131.5+°API)	E –00= g/cm²
bbl × 1.589873	E –01 = m^3
cp × 1.0	E – 03 = Pa.s
ft × 3.048	E – 01 = m
°F (°F-32)/1.8	E – 00 = °C
md × 9.869233	E – 04 = μm^2
psi × 6.894757	E + 00 = KPa

References

1. Gilbert, W .E, : "Flowing and Gas-Lift Well Performance", Drill. and Prod. Prac., API (1954) **126**
2. Vogel, J. V, : "Inflow Performance Relationships for Solution-Gas Drive Wells", ***JPT***,. (January 1968) **83-92**.
3. Weller, W. T, :"Reservoir Performance During Two-Phase Flow", ***JPT*** (Feb, 1966) **240-246**
4. Muskat, M. : **Physical Principles of Oil Production**, Mc Graw-Hill Book Company Inc, New York City (1949).
5. Fetkovich, M. J, : "The Isochronal Testing of Oil Wells", paper SPE 4529 presented at the 1973 SPE Annual Fall meeting, Las Vegas, Nevada, 30 September-3 October.
6. Kniazeff, V. J, and Naville, S. A, : "Two-phase Flow of Volatile Hydrocarbon", **SPEJ** (March 1965) 37; *Trans*., AIME, **234**.
7. Eilerts, C. K. Summer, E. F. and Potts, N. L, : "Integration of Partial Differential Equations for Transient Radial Flow of Gas-Condensate Fluids in Porous Structures", **SPEJ** (June 1965) **141.**
8. Eilerts, C. K. and Summer, E. F, : "Integration of Partial Differential Equations for Multicomponents, Two-phase Transient Radial Flow", **SPEJ** (June 1967) **125.**
9. Gondouin, M., Iffly, R., and Husson, J.:"An attempt to predict the Time-Dependence of Well Deliverabiulity in gas Condensate Fields," SPEJ (June1967) 112; *Trans*.,AIME,**240**
10. O'Dell, H. G, and Miller, R. N, : "Successfully Cycling a Low Permeability, High-Yield Gas Condensate Reservoirs", ***JPT*** (January 1967) **41-44**.
11. Fussell, D.D.: "Single-Well Performance Predictions for Gas-Condensate Reservoirs," JPT (July 1973) 258; *Trans.*, AIME, **255**
12. Dyung, T. Vo, Jones, J., and Raghavan, R : "Performance Prediction for Gas Condensate Reservoir", Paper SPE 16984 first presented at the 1987 SPE Annual Technical Conference and Exhibition held in Dallas, Sept.27-30.
13. Muskat, M. and Meres, M.W.: "The flow of Heterogeneous Fluids Through Porous Media," *Physics* (Sept. 1936) Vol. 7, 346-363.
14. Evinger, H. H, and Muskat, M, : "calculation of Theoretical Productivity factor", Trans, AIME (1942) 146, **126-139**
15. Levine, J.S. and Prats, M.: " The calculated Performance of Solution Gas-Drive Reservoirs," SPEJ (Sept. 1961) 145-152. *Trans*., AIME, Vol. 222
6. Raghavan, R. and Jones, J.R : "Depletion Performance of Gas-Condensate Reservoirs," , ***JPT***,. (August 1996) **725-731**.
16. Fevang, O and Whiston, C. H, : "Modeling Gas-Condensate Well Deliverability", Paper SPE 30714 first presented at the 1995 SPE Annual Technical Conference and Exhibition held in Dallas, 22-25 October.

Table 1 – Reservoir Properties

Permeability, k	50 md
Porosity, ϕ	0.08
Wellbore radius, r_w	0.33 ft
Reservoir extent, r_e	1000 ft
Layer Thickness, h	15.5 ft
Skin, s	0

Table 2 – Relative Permeability Set Generated using a polynamial expression after Kniazeff & Knaville[6]

Sg	krg	kro
0.000000e-001	0.000000e-001	1.000000e+000
2.500000e-002	6.242500e-005	7.169271e-001
5.000000e-002	3.074000e-004	6.115471e-001
3.750000e-001	5.948438e-002	3.738295e-002
4.000000e-001	7.137280e-002	2.637660e-002
4.250000e-001	8.474203e-002	1.743934e-002
4.500000e-001	9.967860e-002	1.024754e-002
4.750000e-001	1.162691e-001	4.517145e-003
5.000000e-001	1.346000e-001	2.500000e-007
5.250000e-001	1.547579e-001	0.000000e-001
5.500000e-001	1.768294e-001	0.000000e-001
5.750000e-001	2.009010e-001	0.000000e-001
8.500000e-001	6.224482e-001	0.000000e-001
8.750000e-001	6.772719e-001	0.000000e-001
9.000000e-001	7.352208e-001	0.000000e-001
9.250000e-001	7.963815e-001	0.000000e-001
9.500000e-001	8.608406e-001	0.000000e-001
9.750000e-001	9.286846e-001	0.000000e-001
1.000000e+000	1.000000e+000	0.000000e-001

Table 3 – Fluid Properties

	Rich Gas Fluid A	**Lean Gas Fluid B**
Initial reservoir pressure (psia)	6000	7400
Dew point pressure (psia)	5214	7350
Reservoir temperature (F)	285	325
Maximum Liquid Dropout during CVD (%)	28	3
Initial CGR (Stb/MMscf)	148	55
Stock-Tank Oil API Gravity	49	45

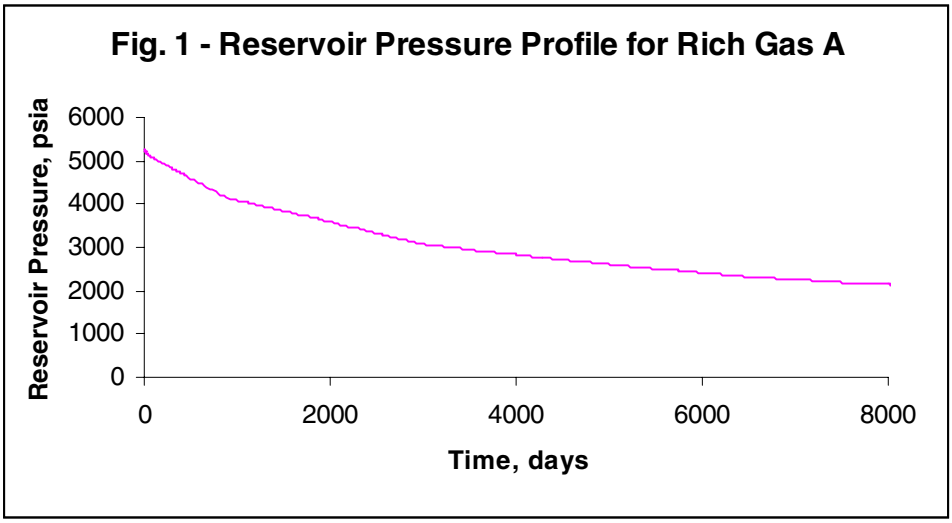
Fig. 1 - Reservoir Pressure Profile for Rich Gas A
Reservoir Pressure, psia
6000
5000
4000
3000
2000
1000
0
0
2000
4000
6000
8000
Time, days

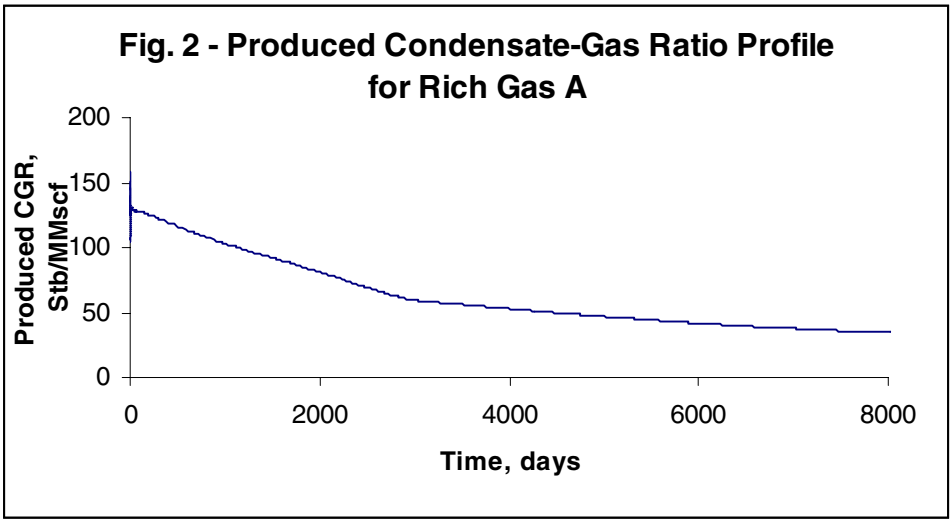
Fig. 2 - Produced Condensate-Gas Ratio Profile for Rich Gas A
Produced CGR, Stb/MMscf
200
150
100
50
0
0
2000
4000
6000
8000
Time, days

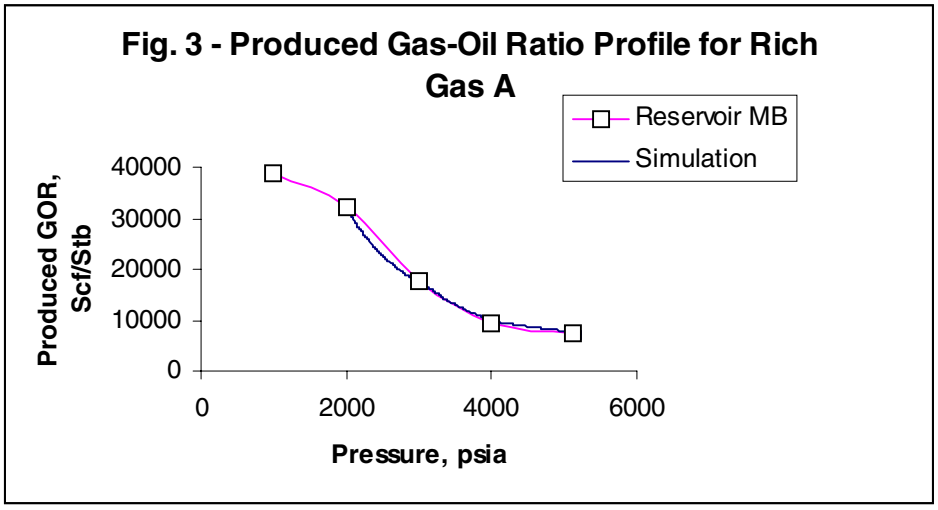
Fig. 3 - Produced Gas-Oil Ratio Profile for Rich Gas A
Reservoir MB
Simulation
Produced GOR, Scf/Stb
40000
30000
20000
10000
0
0
2000
4000
6000
Pressure, psia

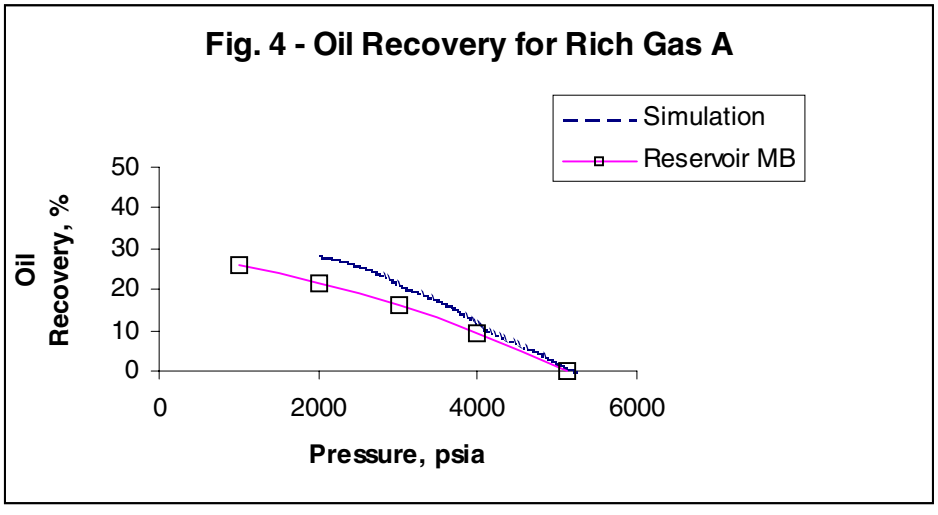
Fig. 4 - Oil Recovery for Rich Gas A
Simulation
Reservoir MB
Oil Recovery, %
50
40
30
20
10
0
0
2000
4000
6000
Pressure, psia

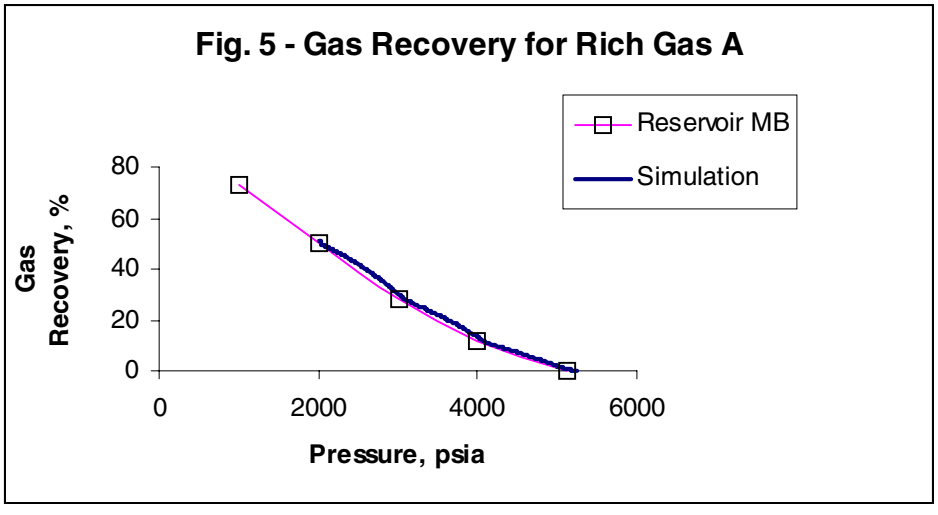
Fig. 5 - Gas Recovery for Rich Gas A
Reservoir MB
Simulation
Gas Recovery, %
80
60
40
20
0
0
2000
4000
6000
Pressure, psia

Fig. 6 - IPR Curves for Rich Gas A

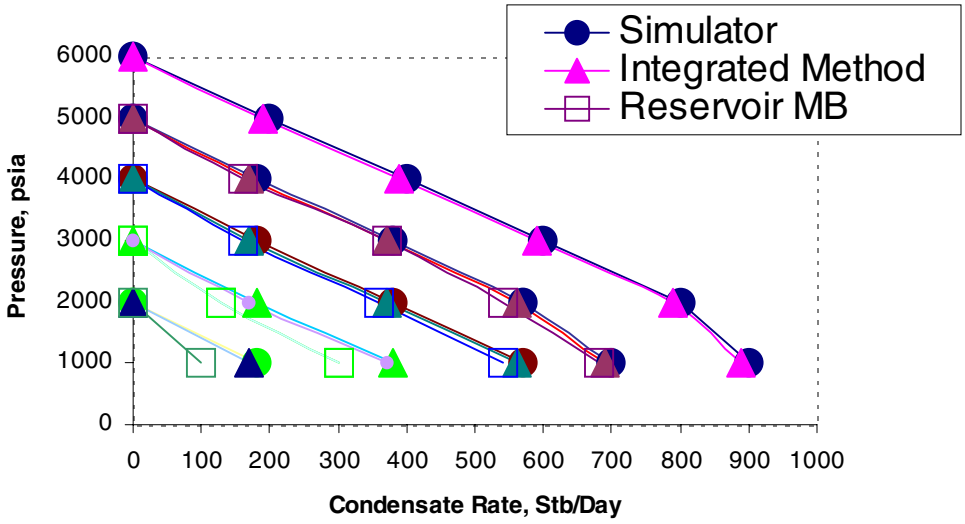

Fig. 7 - IPR Curves for Lean Gas A

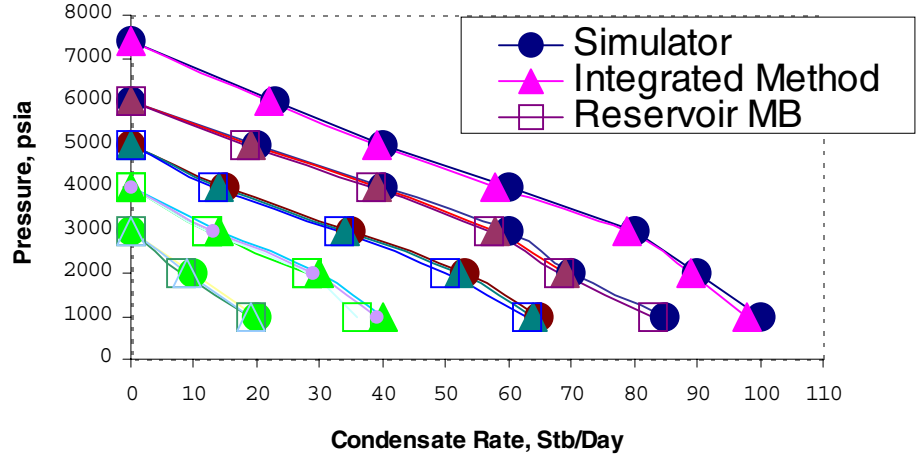
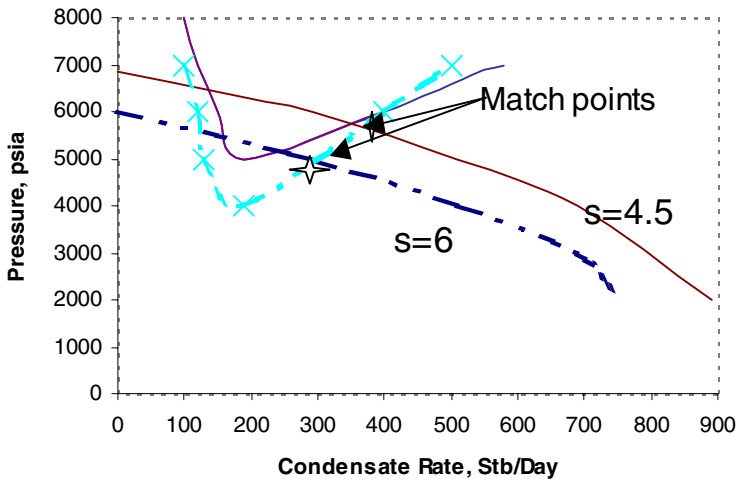
Fig. 8 - West Texas Well Performance